

Edge flame dynamics in a turbulent lifted jet flame

By S. Karami[†], E. R. Hawkes[‡], M. Talei[‡] AND J. H. Chen[¶]

A turbulent lifted slot-jet flame is studied using direct numerical simulation (DNS). A one-step chemistry model is employed with a mixture-fraction-dependent activation energy which can reproduce qualitatively the dependence of laminar burning rate on equivalence ratio that is typical of hydrocarbon fuels. After first describing the overall flame structure, the statistics of flow and relative edge-flame propagation velocity components conditioned on the leading-edge locations are examined. The results show that, on average, the streamwise flame propagation and streamwise flow balance, thus demonstrating that edge-flame propagation is the basic stabilization mechanism. Fluctuations of the edge locations and net edge velocities are, however, significant. It is demonstrated that the edges tend to move in an essentially Two-Dimensional elliptical pattern (starting from a downstream location, laterally outwards towards the oxidizer, then upstream, then inwards towards the fuel, then downstream again). It is proposed that this is due to the passage of large eddies, which is mostly consistent with the picture outlined in Su *et al.* (2006).

1. Introduction

The stability of jet flames is of critical importance in direct injection engines, gas turbines, and many different types of other combustion devices. As a result of a high jet velocity in these devices, the flame is not often attached to the nozzle, but rather it is stabilized at some distance downstream, i.e., it is lifted. The stabilization location strongly influences both emissions and the propensity towards undesirable flame instability.

Therefore, lifted jet flame stabilization has long been a topic of research. Yet, the stabilization mechanism is not fully understood. In the last five decades, various theories have been proposed. These theories may be classified as premixed flame, critical scalar dissipation, edge-flame and large-eddy theories (Lawn 2009). Among these theories, the edge-flame and large-eddy theories have received more attention in the literature. Therefore, brief discussions of these theories are presented below.

The edge-flame stabilization mechanism was initially proposed by Buckmaster & Weber (1996). The edge flame is a partially premixed flame propagating in a quasi-laminar manner with the speed which has the same order of magnitude as the laminar flame speed, and stabilization is achieved when the flow velocity matches this propagation speed. Edge-flame structures have been observed in several experimental studies, for example Stårner *et al.* (1996).

A stabilization mechanism influenced by large-eddy structures was first proposed by Broadwell *et al.* (1985). In this theory, hot products were laterally ejected by large eddies and subsequently re-entrained, which was argued to explain how the flame could retain

[†] School of Photovoltaic and Renewable Energy Engineering, University of New South Wales, Australia

[‡] School of Mechanical and Manufacturing Engineering, University of New South Wales, Australia

[¶] Combustion Research Facility, Sandia National Laboratories

its location at a particular lifted height. Since then, several hybrid theories involving the influence of large eddies have been advanced. Miake-Lye & Hammer (1989) proposed that the flame stabilizes in a region where the strain rate is lower than a critical extinction level, while lifted height fluctuations are controlled by the flame propagating over large eddies. Kelman *et al.* (1998) introduced a concept involving a cyclic motion of edge flames which proceeds via upstream propagation, followed by interaction with a large vortex, leading to extinction and downstream motion until mixture-fraction gradients relax and upstream motion occurs again. Burgess & Lawn (1999) argued that large eddies were mainly a source of external intermittency between turbulent and non-turbulent regions, in which the flame has significantly different burning velocities. For lifted heights larger than 20 diameters downstream, turbulent burning velocities were reasonably consistent with correlations for premixed flames once intermittency was taken into account. For shorter lifted heights, more recent work by Su *et al.* (2006) argued that the basic stabilization mechanism was by edge-flame propagation, with axial and radial fluctuations of edge-flame locations being controlled by the passage of large eddies and the tendency of the flame to maintain a flammable mixture.

The main conclusion from reviews of the literature is that the stabilization mechanism is not fully agreed upon. Edge-flame propagation is widely reported to play a role, and its role is possibly moderated by the presence of large eddies. One reason that these influences have not been fully confirmed is that accurate experimental measurements of the edge-flame relative propagation velocity are lacking. The difficulty is that the measurements are usually planar and the out-of-plane flame structure and propagation speeds are not known. In contrast, direct numerical simulation (DNS) provides simultaneously the full three-dimensional flame structure, flame propagation speeds, and flow velocities, which together are not accessible in current experiments. Therefore, this paper examines interaction of edge flames and turbulent flow in a lifted flame configuration with a view to determining the role of flame propagation and any possible influence of large eddies.

2. Numerical method and simulation parameters

To obtain a realistic parameter space in terms of Reynolds and Damköhler numbers without incurring excessive computational expense, a one-step chemistry model was employed. For a single-step irreversible reaction of $F + rO \rightarrow (1 + r)P$ where r is the stoichiometric ratio, i.e., the mass of oxidant disappearing with unit mass of fuel, the source terms take the following non-dimensional forms

$$\dot{\omega}_F = \frac{1}{r}\dot{\omega}_O = -\text{Da}\rho^2 Y_F Y_O \exp\left[-\frac{\beta(1 - T')}{1 - \alpha(1 - T')}\right], \text{ and } T' = \frac{(\gamma - 1)T - 1}{\tau}, \quad (2.1)$$

where Da is a Damköhler number, α is the heat-release parameter, and β is the Zel'dovich number. To capture qualitatively the strong dependence of the laminar burning velocity on equivalence ratio that is typical of hydrocarbon flames, the activation energy was specified to be mixture-fraction dependent, following Garrido-López & Sarkar (2005).

The conservation equations of mass, momentum, sensible energy, and mass fractions of fuel and oxidiser are nondimensionalised with respect to the inlet jet width, H , the speed of sound, temperature, and thermodynamic properties on the jet centerline at the inlet. These equations are solved in non-dimensional form employing the DNS code S3D.SC which is a modified version of the detailed chemistry code S3D (Chen *et al.* 2009). The solver S3D.SC uses high-order accurate, low-dissipative numerical schemes and a 3D structured, Cartesian mesh. An 8th-order central differencing scheme was used for the spatial derivatives. The time integration was performed with a 6-stage, 4th-order, explicit

TABLE 1. Simulation parameters

Jet width	H
Domain size ($L_x \times L_y \times L_z$)	$16H \times 24H \times 8H$
Number of grid points ($N_x \times N_y \times N_z$)	$800 \times 800 \times 400$
Mean inlet jet non-dimensional velocity (U_{jet})	0.48
Laminar co-flow non-dimensional velocity ($U_{co-flow}$)	0.001
Jet non-dimensional temperature	2.5
Co-flow non-dimensional temperature	2.5
Jet Reynolds number	5,280
Inlet velocity fluctuation	5%
Fuel mixture fraction in fuel stream ($Y_{F,o}$)	1.0
oxidizer mixture fraction in oxidizer stream ($Y_{O,o}$)	0.233
Stoichiometric mixture fraction (Y_{Fst})	0.055
Stoichiometric oxidizer to fuel mass ratio r	4.0
Heat release parameter (α)	0.86
Ratio of specific heat (γ)	1.4
Baseline Zel'dovich number (β_0)	5.0
Non-dimensionisation Damköhler number (Da)	800.0
Prandtl number (Pr)	0.7
Lewis number (Le=Sc/Pr)	1.0

Runge-Kutta method. To suppress numerical fluctuations at high wave numbers, a 10th-order filter was applied every 10 time steps. Non-reflecting outflow boundary conditions (Chen *et al.* 2009) were used in the streamwise and transverse directions, and periodic boundary conditions were applied in the spanwise direction.

The simulation parameters along with their values are presented in Table 1. The configuration is a slot jet flame. The mean inlet axial velocity and fuel mass fraction were specified using a Tanh-based profile. The inlet momentum (and mixing layer) thickness, δ , is equal to $0.05H$. To describe the velocity fluctuations at the inlet, u , a homogeneous isotropic turbulence field based on a prescribed turbulent energy spectrum with a turbulence intensity of 5% is first produced. These velocity fluctuations are then added to the mean inlet velocity and advected into the domain by applying Taylor's hypothesis.

A uniform grid spacing of $0.02H$ was chosen for the streamwise and spanwise directions. An algebraically stretched mesh was applied in the transverse direction which maintained uniform spacing of $0.02H$ in $|y| < 7.5H$ and less than 3% of grid stretching in the region of $|y| > 7.5H$.

The simulation was run for 18.0 jet flow through times, $t_j = L_x/U_j$ (where L_x is the length of the computational domain in the streamwise direction), to obtain a statistically stationary solution, and the data from the last $12.0t_j$ were used for analysis.

The turbulence resolution was assessed considering the Kolmogorov scale defined as $\tilde{\eta}_k = (\tilde{\nu}^3/\tilde{\epsilon})^{1/4}$. The minimum $\tilde{\eta}_k/dx$ at the flame base is roughly 0.5, and most of the time the flame is located in the region of $\tilde{\eta}_k/dx > 0.5$, which is normally considered sufficient for DNS (Pope 2000). Some other studies suggest that at least three grid points within the Kolmogorov length scale is required to obtain a fully resolved DNS (Hamlington *et al.* 2008). However, this will significantly increase the cost of the turbulent lifted flame, by a factor of more than 1000, so as to make such a well-resolved simulation impractical at the present time. To give an indication of the flame resolution, a symmetric triple flame was simulated using the same parameters as the turbulent case. The thermal thickness was defined as $\delta_{th} = (T_{ad} - T_o)/(\partial T/\partial \xi)$, where T_{ad} is the adiabatic flame temperature,

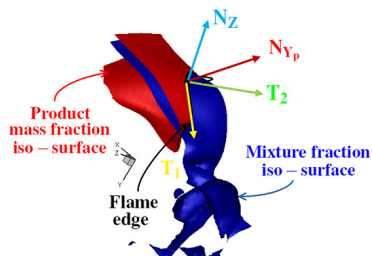


FIGURE 1. Various normal and tangential vectors at the flame base. The red surface is the product mass fraction iso-surface, the blue surface is the mixture-fraction iso-surface, and the solid black line is the edge-flame.

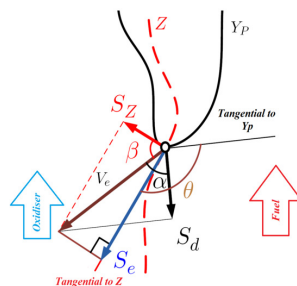


FIGURE 2. Schematic of edge-flame propagation along the mixture-fraction iso-surface.

T_o is the unburned mixture temperature, and ξ is the mixture fraction corresponding to the maximum laminar flame speed. The thermal thickness was equal to $0.16 H$, and there are 8 grid points across the flame, which is normally considered sufficient for a one-step chemistry DNS (Chakraborty & Mastorakos 2008). Extensive visualisations of the structures observed in the DNS revealed comparable resolution of the edge-flame structures.

3. Mathematical background

We now develop some necessary background regarding the identification of flame edges and their speeds relative to the flow.

Analyzing edge-speed statistics requires some way to identify the flame edges. In premixed combustion, flame speeds are frequently obtained by calculating the displacement speed of a reacting scalar at a location in the flame that approximately tracks the locations of peak heat release (Hawkes *et al.* 2007). In partially premixed flame edges the situation is more complicated. Observations from DNS (Pantano 2004; Hawkes *et al.* 2007) show that the flame edges tend to remain anchored near to a particular mixture-fraction iso-surface. Therefore, following earlier studies of extinction and reignition (Pantano 2004; Hawkes *et al.* 2007), we select a flame-edge marker that is the intersection of a mixture-fraction iso-surface and a product mass-fraction iso-surface †.

To choose the mixture-fraction iso-surface, it is presumed that the leading edge will be found at the mixture fraction corresponding to the largest laminar flame speed, which is slightly rich of stoichiometric (0.07 in this study). To select the product mass-fraction iso-surface, a one-dimensional (1D) simulation of a laminar premixed flame with the same flame parameters as the turbulent lifted flame was performed. The product mass fraction Y_p corresponding to the location of maximum heat release rate was obtained from this simulation as 0.2. In the 3D DNS, the results were extensively visualized, and it was found that this definition reliably tracked the leading edges of the flame as well as edges around local flame holes, as judged by comparison with regions of peak reaction rate.

To analyze the edge-flame motion, a coordinate system moving with the flow velocity

† With this definition, the edge-flame propagation speed can be theoretically linked to a source term in the evolution equation of the flame surface-area density of the stoichiometric surface conditioned upon the reacting scalar (Hawkes *et al.* 2007). An investigation of this transport equation is left for future work.

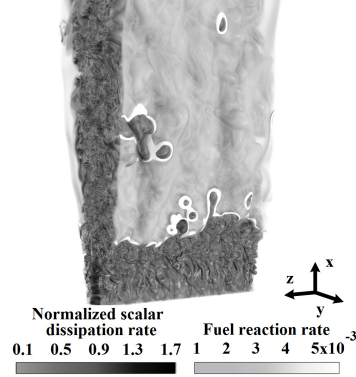


FIGURE 3. Three-dimensional volume rendering of the logarithm of the scalar dissipation rate (gray/black) and reaction rate (white/light gray). (Only the region $x < 14$ is shown.)

is first defined - see Figure 1. In Figure 1, the normal to the mixture-fraction iso-surface is denoted \mathbf{N}_Z (pointing towards oxidizer); the normal to the product mass-fraction iso-surface is denoted \mathbf{N}_{Y_p} (pointing towards reactants); the tangent to the mixture-fraction iso-surface which points along the flame edge is denoted \mathbf{T}_1 ; and finally, the tangent to the mixture-fraction iso-surface which is normal to \mathbf{T}_1 , and pointing towards the reactants, is denoted \mathbf{T}_2 . It is readily shown that these quantities are given by

$$\begin{aligned} \mathbf{N}_Z &= -\frac{\nabla Z}{|\nabla Z|}, & \mathbf{N}_{Y_p} &= -\frac{\nabla Y_p}{|\nabla Y_p|}, \\ \mathbf{T}_1 &= \frac{\mathbf{N}_{Y_p} \times \mathbf{N}_Z}{|\mathbf{N}_{Y_p} \times \mathbf{N}_Z|}, & \text{and } \mathbf{T}_2 &= \frac{\mathbf{N}_Z \times (\mathbf{N}_{Y_p} \times \mathbf{N}_Z)}{|\mathbf{N}_{Y_p} \times \mathbf{N}_Z|}. \end{aligned} \quad (3.2)$$

Figure 2 shows a schematic, in the plane containing both \mathbf{N}_Z and \mathbf{N}_{Y_p} , of the edge-point motion. Because the chosen coordinate system moves with the local flow velocity, only the motion of the iso-surfaces relative to the flow need be considered. Relative motion is a result of relative displacement of both the mixture-fraction and product mass-fraction iso-surfaces. The mixture-fraction iso-surface moves with velocity $S_Z \mathbf{N}_Z$, while the $Y_P = Y_P^*$ iso-surface moves with velocity $S_d \mathbf{N}_{Y_p}$, where the displacement speeds are given as Pope (1988)

$$\begin{aligned} S_Z &= \frac{1}{\rho |\nabla Z|} \left(-\frac{\partial}{\partial x_j} \left(\frac{\mu}{Sc} \frac{\partial Z}{\partial x_j} \right) \right), \text{ and} \\ S_d &= \frac{1}{\rho |\nabla Y_P|} \left(-\dot{\omega}_P - \frac{\partial}{\partial x_j} \left(\frac{\mu}{Sc} \frac{\partial Y_P}{\partial x_j} \right) \right). \end{aligned} \quad (3.3)$$

We denote the overall velocity of the edge point \mathbf{V}_e and break this down in the orthonormal coordinates \mathbf{N}_Z and \mathbf{T}_2 as

$$\mathbf{V}_e = S_Z \mathbf{N}_Z + S_e \mathbf{T}_2, \quad (3.4)$$

where $S_e = \mathbf{V}_e \cdot \mathbf{T}_2$ is the projection of \mathbf{V}_e into the plane of the mixture-fraction iso-surface and needs to be determined. By taking the dot product of Eq. 3.4 with \mathbf{N}_{Y_p} , it is readily shown that

$$S_e = \frac{S_d - k S_Z}{\sqrt{1 - k^2}}, \quad (3.5)$$

where k is the inner product of the normal vectors $\mathbf{N}_{Y_p} \cdot \mathbf{N}_Z$. Although the presentation here is slightly different, it has been verified that the final result is the same edge speed used first by Pantano (2004) to study extinction holes, and later by Hawkes *et al.* (2007)

to study extinction and reignition, as well as Chakraborty & Mastorakos (2008) to study ignition.

Later in the paper, the flame stabilization mechanism will be examined considering the motion of edge flames in an ensemble of two-dimensional streamwise-transverse planes. As a result of the reduction to two dimensions, the effects of out-of-plane motion need to be considered in the treatment of the averaged edge-flame velocities in each plane. The out-of-plane components are readily determined by projecting the out-of-plane velocities as

$$\begin{aligned} U_{z,x} &= -U_z \tan(\varphi) \cos(\psi), \quad U_{z,y} = -U_z \tan(\varphi) \sin(\psi), \\ (V_{e,z})_x &= -V_{e,z} \tan(\varphi) \cos(\psi), \quad \text{and } (V_{e,z})_y = -V_{e,z} \tan(\varphi) \sin(\psi), \end{aligned} \quad (3.6)$$

where U_z and $V_{e,z}$ are the spanwise components of the flow velocity and flame propagation, respectively; φ is the angle between the edge-flame tangent \mathbf{T}_1 and the $x - y$ plane; and ψ is the angle between the projection of \mathbf{T}_1 in the $x - y$ plane and the x -axis.

4. Results and discussion

4.1. General structure

A volume rendering of logarithm of the scalar dissipation rate normalized by laminar flame time-scale (gray/black) and reaction rate (white/light gray) is presented in Figure 3. Note that the leading flame edges at the base of the flame (the bright white regions) are highly convoluted. Consistent with many experimental observations of lifted flames (Su *et al.* 2006; Lawn 2009; Kelman *et al.* 1998), the leading edges do not typically exhibit a tribrachial structure. This lack of three distinct branches has been previously explained to result from mixture-fraction gradients ahead of the flame being too large to support distinct lean and rich branches (Stärner *et al.* 1996). Occasionally, when the flame is found in a low strain-rate region, we did observe a short or weak rich premixed branch, but a distinct lean branch was never observed.

The reaction rate is locally higher at the flame edges than further downstream, which is consistent with the existence of a partially premixed leading –edge flame. Note also, in the present case, the edge flames are quite narrow and of the order of the laminar flame thickness, which implies that they are quite unlike a flat turbulent premixed flame with lateral dimensions much larger than the laminar flame thickness, i.e., at this lifted height, the premixed flame theory of stabilization is ruled out, a fact which has already been noted by others, e.g., see the discussion in Lawn (2009).

Unlike the DNS of lifted hydrogen flames reported by Mizobuchi *et al.* (2005), we do not observe a vigorous rich premixed flame core. Similarly, we also did not observe any diffusion flame islands on the lean side observed by Mizobuchi *et al.* (2005). We believe these differences are attributable to the fact that hydrogen burns much more vigorously than hydrocarbons in rich mixtures. Here, the mixture-fraction-dependence of the burning velocity is built into the present model by the mixture-fraction- dependent activation energy.

4.2. Flame propagation statistics

The means and PDFs of the net edge-flame velocities (flow plus flame propagation) conditional on streamwise distance are shown in Figures 4(a)-(c). Before discussing the more interesting streamwise and transverse components, note that the spanwise net velocity component has an approximately zero mean, as expected, with a PDF that is approximately symmetric about the mean, and a width that is significant relative to the other components (corresponding to a similar level of velocity fluctuations).

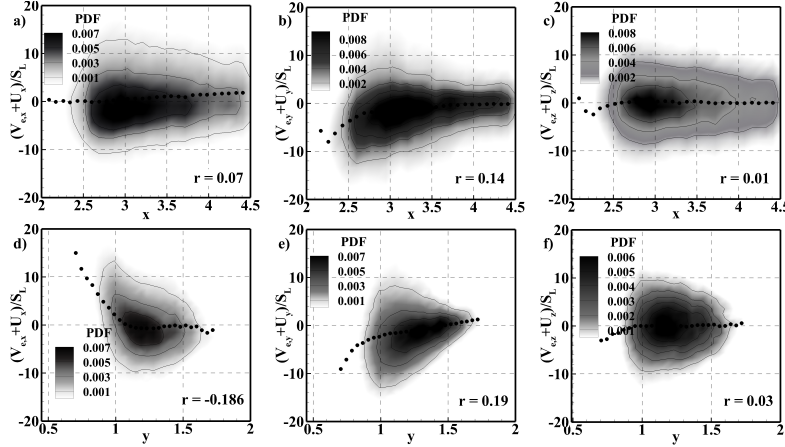


FIGURE 4. Net flame velocity components conditioned on the edge-flame locations (including both flow and flame propagation velocities), showing: (a,b,c) contour plots of the joint PDFs of the net velocity components and streamwise location of the flame edge and the streamwise conditional mean net velocities; and (d,e,f) the joint PDFs of the net velocity components and transverse location and corresponding conditional means.

Here, Figure 4(a) shows that the streamwise flow velocity on average balances the streamwise upstream flame propagation in the most probable regions of flame stabilization. This demonstrates that the flame is stabilized by edge-flame propagation, which is a major result of the paper. Note that there is some lack of balance in the downstream regions starting from about $x \approx 3.5$. This is probably connected with flame holes which move further downstream before they are annihilated.

Moving on to the transverse net velocity conditional on streamwise distance shown in Figure 4(b), note that the conditional mean of the flow plus flame propagation velocity does not balance in the upstream region, where on average the flame is entrained into the jet core.

Similarly, while the streamwise net velocity conditioned on transverse distance shown in Figure 4(d) has a conditional mean which is close to zero at larger y values, it is strongly positive towards the core of the jet, indicating that the flame must move downstream in this region. Finally, the transverse net velocity conditioned on transverse distance is shown in Figure 4(e). It has an overall positive correlation and, interestingly, presents the most negative transverse velocities (i.e., towards the jet core) at small transverse locations.

Summarizing these results, although the streamwise net velocity conditioned on streamwise distance is close to zero, the flame appears to move inwards at upstream locations, where it experiences increasingly rapid inwards and downstream motion. As a result, based only on the means conditional on streamwise or transverse distance, there does not appear to be a way to explain how flames escape the inner high-velocity region. In the below, we show that this is because the stabilization mechanism is fundamentally two dimensional.

We now consider the two-dimensional picture. We consider the on-average apparent motion of the edge flames in the ensemble of all $x - y$ planes, averaging in the spanwise direction and in time. As we consider the motion of edge flames in the plane, the effect of the out-of-plane motion needs to be considered, and therefore we employ the net edge-flame velocities, including the contributions of out-of-plane motion (as per Eq. (3.7)). In

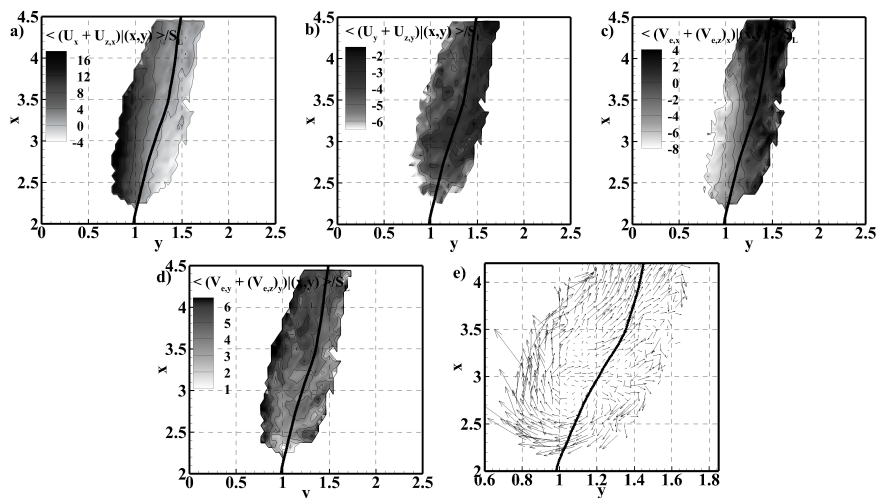


FIGURE 5. The following quantities, conditionally averaged on both streamwise and transverse locations of the instantaneous flame base, and including the components due to out-of-plane flow and/or propagation: (a) streamwise flow velocity; (b) transverse flow velocity; (c) the streamwise edge propagation velocity; (d) the transverse edge propagation velocity; and e) the vectors of the relative velocity. The solid line is the temporally and spatially Favre-averaged mixture fraction equal to 0.07.

what follows, we will show that the flame tends, on average, to move sequentially around its mean location. The flame moves first upstream, then inwards, then downstream, and finally outwards. Viewing the flame in the z -direction, this motion is clockwise on the right-hand side and anti-clockwise on the left-hand side of the jet. Figures 5(a,b) show the flow velocities in the streamwise and transverse directions, respectively, with the out-of-plane components added in, while Figures 5(c,d) show the corresponding relative flame propagation velocities. In discussing these Figures below, we refer to the lean and rich side, by which we mean the on-average lean or rich side, recalling that the instantaneous edge flames are always located on a fixed mixture-fraction iso-surface.

In considering the flow velocities, the streamwise component is mostly negative (i.e., upstream) on the lean side and mostly positive (i.e., downstream) on the rich side. The transverse component is negative everywhere, but most strongly so at upstream locations and on the lean side. The relative propagation velocity in the streamwise direction is strongly upstream on the lower left side, whereas it is in the downstream direction on the upper right side. The relative propagation velocity in the transverse direction is generally outwards, counter acting the inwards entraining flow. Adding the flow and flame propagation velocities together results in the net velocities shown as vectors in Figure 5(e), which clearly shows a nearly complete clockwise rotation around the region of the most likely stabilization point.

There is one caveat; the flame edges that are located further downstream than $x \approx 3.5$ tend to continue to move downstream. It is suggested that these are due mainly to flame holes, or to segments of the flame edge that are about to break off and become holes, which were not conditioned out of this analysis.

It is proposed that the above elliptical pattern of motion is connected to the passage of large eddies. Starting from a downstream location on the stoichiometric line, a clockwise-rotating large eddy arrives and moves the flame first outwards towards the lean side, then upstream, while the flame moves inwards to maintain a stoichiometric mixture. As the

large eddy passes, the flame is then rapidly entrained by the eddy into the jet core, where it experiences high streamwise velocity and again moves downstream. Among various works that describe influences of large eddies, the present findings are most consistent with the picture outlined by Su *et al.* (2006), which connects the fluctuations of the edge-flame location with large-scale jet organization.

5. Conclusion

A direct numerical simulation of a lifted, slot-jet flame in a cold oxidizer environment has been presented. To achieve a relevant parameter space in terms of Reynolds and Damköhler numbers, a simple one-step chemistry model was used with an adjusted activation energy that qualitatively reproduces the strong equivalence ratio dependence of burning velocity which is typical of hydrocarbon flames.

The overall structure of the flame was first examined. The flame was found to involve a highly convoluted leading edge-flame structure and a trailing non-premixed flame exhibiting some flame holes. Holes are initiated by two different mechanisms. Some of the holes are generated by flame propagation at the leading edge while others are caused by local flame extinction. The extinction holes are due to high scalar dissipation rate. At the instant of the hole creation, the scalar dissipation rate is high, while during the healing process, the scalar dissipation rate relaxes and the edge flame can propagate and close the hole. The process of opening and closing the holes and its dependency on turbulence and thermo-chemistry parameters is left for future work.

The leading-edge flames were found to be composed primarily of a single branch centred close to the stoichiometric mixture-fraction surface – lean branches were never observed and rich premixed branches were rarely observed. In contrast, previous hydrogen lifted-flame DNS observed a vigorous inner rich premixed flame, which may be connected to the rather different flammability limits of hydrogen as compared with hydrocarbons. No evidence of unconnected flame elements was observed either as disconnected pockets of products upstream of the main flame or, in contrast to previous hydrogen lifted-flame DNS, as diffusion flame islands in lean regions.

The statistics of flow and edge-flame propagation velocity components conditioned on the instantaneous locations of the flame revealed that the flow, on average, balances the relative propagation in the streamwise direction, thus demonstrating that the flame is stabilized essentially by edge-flame propagation. To the best of our knowledge, this is the first such demonstration, in a turbulent lifted flame, employing local flame propagation speeds with all velocity and flame propagation components included.

There are significant fluctuations in lifted height, and conditioning of the net flame velocity on streamwise and transverse locations revealed an elliptical pattern of flame motion around the average stabilization point. It was proposed that this motion is connected with the passage of large eddies, which was mostly consistent with a picture previously proposed by Su *et al.* (2006). Overall, the results provide strong support for the edge-flame theory of lifted flame stabilization, with large eddies playing a key role in lifted height fluctuations.

Acknowledgments

This work was supported by the Australian Research Council. Use of the facilities of the Center for Turbulence Research (CTR) at Stanford University during the 2014 Summer Program is gratefully acknowledged. The research also benefited from computational resources provided through the National Computational Merit Allocation Scheme, supported by the Australian Government. The computational facilities supporting this

project included the Australian NCI National Facility and the partner share of the NCI facility provided by Intersect Australia Pty, Ltd.

REFERENCES

- BROADWELL, J. E., DAHM, W. J. & MUNGAL, M. G. 1985 Blowout of turbulent diffusion flames. *Symp. (Int.) Combust.* **20**, 303–310.
- BUCKMASTER, J. & WEBER, R. 1996 Edge-flame-holding. *Symp. (Int.) Combust.* **26**, 1143 – 1149.
- BURGESS, C. P. & LAWN, C. J. 1999 The premixture model of turbulent burning to describe lifted jet flames. *Combust. Flame* **119**, 95–108.
- CHAKRABORTY, N. & MASTORAKOS, E. 2008 Direct numerical simulations of localised forced ignition in turbulent mixing layers: The effects of mixture fraction and its gradient. *Flow Turbul. Combust.* **80**, 155–186.
- CHEN, J., CHOUDHARY, A., DE SUPINSKI, B., DEVRIES, M., HAWKES, E., KLASKY, S., LIAO, W., MA, K., MELLOR-CRUMMEY, J., PODHORSZKI, N., SANKARAN, R., SHENDE, S. & YOO, C. 2009 Terascale direct numerical simulations of turbulent combustion using S3D. *Comput. Sci. Discov.* **2**, 015001.
- GARRIDO-LÓPEZ, D. & SARKAR, S. 2005 Effects of imperfect premixing coupled with hydrodynamic instability on flame propagation. *Proc. Combust. Inst.* **30**, 621 – 628.
- HAMLINGTON, P. E., SCHUMACHER, J. & DAHM, W. J. 2008 Local and nonlocal strain rate fields and vorticity alignment in turbulent flows. *Phys. Rev. E* **77**, 026303.
- HAWKES, E., SANKARAN, R. & CHEN, J. 2007 Reignition dynamics in massively parallel direct numerical simulations of CO/H_2 jet flames. In *16th Australasian Fluid Mechanics Conference (AFMC)*, pp. 1271–1274. The University of Queensland.
- KELMAN, J. B., ELTOBAJI, A. J. & MASRI, A. R. 1998 Laser imaging in the stabilisation region of turbulent lifted flames. *Combust. Sci. Technol.* **135**, 117–134.
- LAWN, C. J. 2009 Lifted flames on fuel jets in co-flowing air. *Prog. Energy Combust. Sci.* **35**, 1–30.
- MIAKE-LYE, R. C. & HAMMER, J. A. 1989 Lifted turbulent jet flames: A stability criterion based on the jet large-scale structure. *Proc. Combust. Inst.* **22**, 817–824.
- MIZOBUCHI, Y., SHINIO, J., OGAWA, S. & TAKENO, T. 2005 A numerical study on the formation of diffusion flame islands in a turbulent hydrogen jet lifted flame. *Proc. Combust. Inst.* **30**, 611–619.
- PANTANO, C. 2004 Direct simulation of non-premixed flame extinction in a methane-air jet with reduced chemistry. *J. Fluid Mech.* **514**, 231–270.
- POPE, S. 1988 The evolution of surfaces in turbulence. *Int. J. Eng. Sci.* **26**, 445–469.
- POPE, S. B. 2000 *Turbulent Flows*. Cambridge University Press.
- STÄRNER, S. H., BILGER, R. W., FRANK, J. H., MARRAN, D. F. & LONG, M. B. 1996 Mixture fraction imaging in a lifted methane jet flame. *Combust. Flame* **107**, 307–313.
- SU, L. K., SUN, O. S. & MUNGAL, M. G. 2006 Experimental investigation of stabilization mechanisms in turbulent, lifted jet diffusion flames. *Combust. Flame* **144**, 494–512.